Available online at www.sciencedirect.com
SCIENCE DIRECT®
Il Farmaco 58 (2003) 883–889
IL FARMACO
www.elsevier.com/locate/farmac

Structural characterization of a dipeptide compound with immunostimulant activity: 3-(5-thioxo-L-prolyl)-L-thiazolidine-4-carboxylic acid

R. Artali [a], G. Bombieri [a,*], F. Meneghetti [a], D. Nava [b], E. Ragg [c], R. Stradi [b]

[a] *Istituto di Chimica Farmaceutica e Tossicologica, Viale Abruzzi, 42, I-20131 Milano, Italy*
[b] *Istituto di Chimica Organica 'Alessandro Marchesini', Via Venezian, 21, I-20133 Milano, Italy*
[c] *Dipartimento di Scienze Molecolari Agroalimentari, Via Celoria, 2, I-20133 Milano, Italy*

Received 18 December 2002; accepted 19 April 2003

Abstract

The structural characteristics of an immunostimulating agent (3-(5-thioxo-L-prolyl)-L-thiazolidine-4-carboxylic acid) have been established using a combination of ^{1}H and ^{13}C NMR spectroscopy, molecular mechanic calculations (in vacuo and in solution) and X-ray crystallographic analyses. Conformational calculations and NMR spectra identify two classes of conformers, cis and trans, around the peptide bond between the rings, while in the solid state only the cis form has been found.

Keywords: Proline dipeptides; Immunostimulating agents; Structural studies

1. Introduction

The synthetic dipeptide 3-L-(5-oxo-L-prolyl)-L-thiazolidine-4-carboxylic acid (**1**) is an immunostimulating agent used in the treatment of primary or acquired immunodeficiencies and recurrent infection diseases [1]. Its 5-thioxo isoster 3-(5-oxo-L-prolyl)-L-thiazolidine-4-carboxylic acid (**2**), easily prepared from **1** using as thionating agent the Lawesson's reagent in aprotic solvents 2a[2b] has shown interesting immunostimulating, antitoxic, antiradical, and antiagening activities. In fact this molecule administered by oral route in rats at 0.5 mg/kg gave 60–70% protection against formaldehyde-induced toxicity and also reduced doxorubicin-induced mortality in mice. The immunostimulating activity of this compound, evaluated using the test of superoxide anion production in prednisolone-immunodepressed murine peritoneal macrophages [3] is higher than **1**.

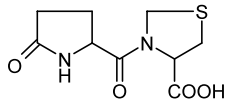

Compound **1**

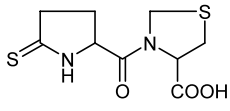

Compound **2**

A previous theoretical study of **1** [4], also associated with NMR spectra [5], identify two classes of conformers trans and cis around the peptide bond with a close conformational population (55 and 45%, respectively), while the X-ray analysis proved that the conformation of the molecule in solid state is cis and with an absolute configuration (2S, 5R). Here, we report on a theoretical study on compound **2** using a combination of molecular and quanto-mechanics analysis. The results are discussed with the experimental data obtained by NMR spectroscopy and X-ray analysis on single crystal and compared with those obtained for compound **1** in order to have a better understanding of the activity structure relationships in the two compounds.

* Corresponding author.
E-mail address: gabriella.bombieri@unimi.it (G. Bombieri).

0014-827X/03/$ - see front matter © 2003 Published by Éditions scientifiques et médicales Elsevier SAS.
doi:10.1016/S0014-827X(03)00146-0

2. Results and discussion

The molecular structure of **2** with the atom numbering scheme is shown in Fig. 1. The thiazolidine and the prolyl rings are rotated by 87.4(1)° while the carboxylic group is rotated of 79.3(1)° with respect to the attached thiazolidine moiety. The thiazolidine is present in envelope conformation, while in the oxo-derivative two conformations (envelope and quasi-planar) were observed due to two alternative disordered positions of the sulfur atom with respective population of 80 and 20%, respectively. The prolyl ring has puckering parameters ϕ: −152.2(9)° and $Q = 0.183(3)$ Å indicative of a twisted conformation.

The torsion angles φ_1, −132.9(3)° [−88.2(2)°]; φ_2, −4.4(4)° [−2.4(3)°]; and φ_3, −52.1(6)° [−88.7(3)°] (φ_1, [N(1)–C(4)–C(5)–C(6)]; φ_2, [C(3)–N(1)–C(4)–C(5)]; and φ_3, [C(1)–C(2)–C(9)–O(1)) are significantly different from those of the oxoderivative (reported in square brackets) as evidenced in Fig. 2 where the two molecules are superimposed along the dipeptide bond. In Fig. 3, the two single molecules are reported for sake of clarity. The conformational differences between the two compounds are reflected in the crystal packing with different intermolecular hydrogen bonds as shown in Fig. 4. In this case the peptidic oxygen O(3) is acceptor of a proton of the hydroxyl group O(2)–H(21)···O(3)′ of 1.86 Å and angle of 168(3)° (′ at 1/2+x, 1/2−y, 1−z), while in the oxoderivate the hydroxyl group is in contact with the carbonyl oxygen of an adjacent prolyl moiety. The nitrogen proton interacts with the sulphur S(2)″ with N(2)···S(2)″ separation of 3.325(3) Å and N(2)–H(22)···S(2)″ 2.59(4) Å with relative angle of 148(3)° (″ at −x, 1/2+y, 1.5−z). Significant intermolecular distances are also C(3)–H(31)···O(3)‴ 2.32(4) Å with an angle of 170(3)° (‴ at 1+x, y, z), C(7)–H(71)···O(1)^{IV} 2.66(4) Å with an angle 150(3)° (^{IV} at −1/2+x, 1/2−y, 1−z) and C(2)–H(2)···S(1)^{V} 2.65(4) Å with an angle of 141(3)° (^{V} at −1+x, y, z).

The conformation of the acidic form of the molecule in the solid state is cis and its absolute configuration (2S, 5R) has been assigned on the basis of the crystallographic results and it corresponds to that observed in solution from NOE experiment. In the oxoderivative the absolute configuration was assigned by the chemical pathway followed in the preparation of the compound.

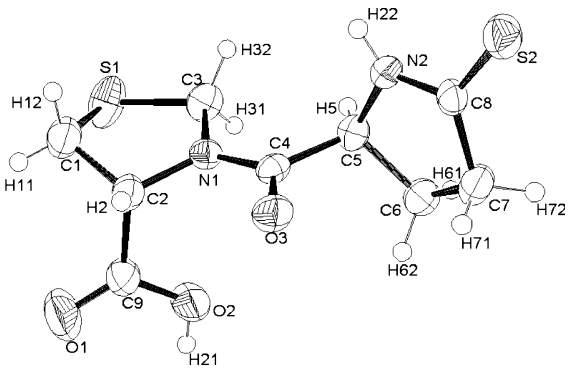

Fig. 1. ORTEP [11] drawing of compound **2**. (Ellipsoids are at 50% probability.)

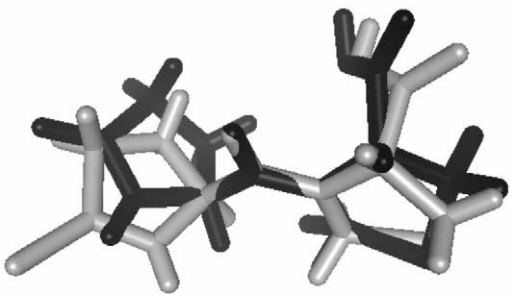

Fig. 2. Superimposition of the crystallographic structures of compounds **1** (black) and **2** (grey).

A parallel study by NMR spectroscopy was performed in order to characterize the possible conformers present in solution.

In analogy with the parent compound all ^{1}H and ^{13}C resonances were found splitted in two groups of signals with a 7:3 intensity ratio, suggesting that the molecule is present in dimethylsulfoxide solution in two main conformations, with different populations. The exchange rate between the two conformers is slow on the NMR time scale and is due to the restricted rotation of the thiazolidine moiety around the CO–N bond.

In order to establish the relative orientation of the two rings in both major and minor rotamers, 2D-NOESY experiments were performed at room temperature with different values of mixing-time, allowing the measurement of through-space interactions between protons at a distance less than 4 Å. Sign and intensity of the NOE cross-peaks depend on the molecular correlation time. For small molecular weight molecules NOE interactions have opposite sign with respect to the diagonal and are therefore clearly distinguishable from the exchange cross-peaks, which are always of the same sign. Fig. 5 shows some traces relative to proton resonances residing on the thiazolidine and on the prolyl rings in the major (trace A) and minor conformer (trace B). The strong negative peaks close to the diagonal are due to chemical exchange, while the positive interactions are true NOE peaks. Trace A shows the geminal interaction between the methylene protons C3–H_a and C3–H_b and proves their proximity in space with the methylene group in positions 6. This allows the identification of conformer A as the major rotamer (see Scheme). In the same trace it is evident also a positive interaction involving C3–H_a of conformer B. This is due to transferred-NOE from C3–H_b(B), whose resonance was saturated by chemical exchange from C3–H_b(A). Trace B shows the through-space interactions of C2–H(B) with C1–H(B) and C5–H(B). The first one is due to a vicinal interaction, while

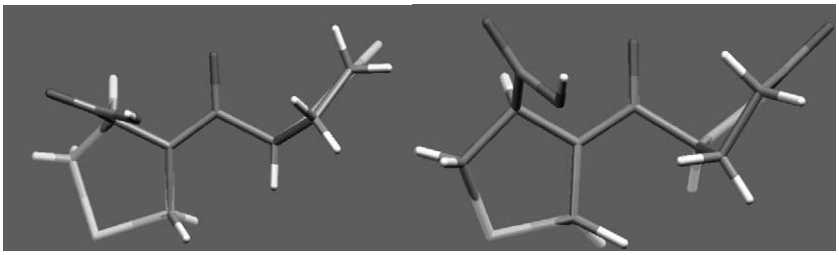

Fig. 3. Plane of the peptidic bond in compound **1** (left) and in **2** (right).

the second one is due to the spatial relationship between protons residing on the two rings and characterizes conformer B. Also in this trace is evident a transferred-NOE involving protons C2–H and C1–H of conformer A.

Compound **2** was also studied by molecular mechanics in vacuo and in solution. The conformers population obtained indicates a predominance of the trans conformers (ratio trans–cis 1.9) enforced by the formation of an intramolecular hydrogen bond between

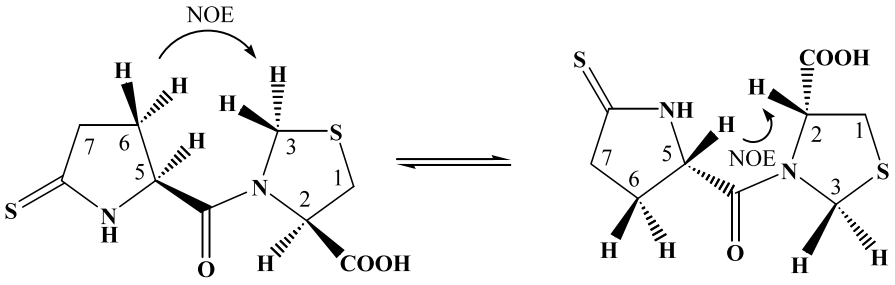

From Table 1, it is evident that the two conformers do not possess identical vicinal coupling constants. In particular, the coupling constants between C2–H and C1–H_a and between C2–H and C1–H_b are significantly different. The first coupling assumes values of 7.4 and 6.1 Hz, respectively for conformers A and B, while the second one, equal to 4.1 Hz in A, decreases down to 1.2 Hz in conformer B. This is a clear indication of an additional conformational averaging inside the prolyl ring, which in turn is dependent on the cis–trans isomerism. Actually, the overall conformation of the molecule is defined not only by the puckering of the pentatomic rings, but also by the two φ_1 and φ_2 torsional angles at the level of the carbonyl group connecting the two rings. The conformation of the prolyl ring seems quite fixed, whereas the thiazolidine ring is characterized by an extensive internal mobility observed also in solid state as shown in the oxo and thio derivatives.

the carboxylic oxygen and the N(2) proton of the prolyl moiety as shown in Fig. 6. The proton distances measured between C6–H_2 and C3–H_2 ($d = 2.3$ Å for hydrogen pairs situated at the minimum distance) and between C5–H and C3–H ($d = 2.5$ Å), respectively for the cis and trans conformers (see Scheme), are in agreement with the NOE interactions observed in the NMR experiments. In addition, among the possible cis isomers, the one at lower energy has a torsion angle φ_2 of $-3.8(3)^\circ$ in agreement with the experimental value (X-ray) of $-4.3(3)^\circ$. Then it is possible to assume that the different conformation found in the solid state, cis with respect to the trans indicated by theoretical investigations, can be related to the intermolecular interactions stabilizing the cis form with respect to the trans (see Fig. 4). This seems confirmed by an additional study QM/MM carried out with the deprotonated carboxylate soaked in water, which results are opposite to those in vacuo, showing how the formation of

Table 1
^{1}H, ^{13}C NMR chemical shifts [a] (δ/ppm) and proton coupling constant values [b] ($J_{H,H}$/Hz) in DMSO-d_6

Position	Rotamer A			Rotamer B		
	δ (^{1}H)	δ (^{13}C)	$J_{H,H}$	δ (^{1}H)	δ (^{13}C)	$J_{H,H}$
C1–H_a	3.35	32.72	7.4,11.7	3.31	34.47	6.1, 11.3
C1–H_b	3.12		11.7, 4.1	3.38		11.3, 1.2
C2–H	4.86	62.01	7.4, 4.1	5.03	61.56	6.1,1.2
C3–H_a	4.88	48.37	8.4	4.60	48.75	9.5
C3–H_b	4.47		8.4	4.33		9.5
C5–H	4.92	62.57	5.1, 9.1	4.65	63.24	4.8, 8.8
C6–H_a	2.48	27.08	n.d.	2.52	27.95	n.d.
C6–H_b	2.00		n.d.	1.91		n.d.
C7–H_a,C7–H_b	2.73, 2.73	43.55	n.d.	2.69, 2.69	43.55	n.d.
N2–H	10.28	–	<1	10.27	–	<1

[a] ppm values at 298 K from TMS. Estimated accuracy within $\pm$0.01 ppm.
[b] From first-order analysis. Estimated accuracy $\pm$0.2 Hz.

intermolecular hydrogen bonds (due to the solvation) can favor the cis conformation with respect to the trans.

Summing up the elongated molecular shape of the cis form found in the solid state (X-ray data) stabilized by the intermolecular hydrogen bonds, previously described, agrees with the findings of the NMR and QM/MM studies in solution, indicating the preference for this conformation. These results indicate that the cis conformation should be preferred in the interaction with the receptor site.

Analogous conclusions have been drawn in a theoretical study of the parent compound PIDOTIMOD [12].

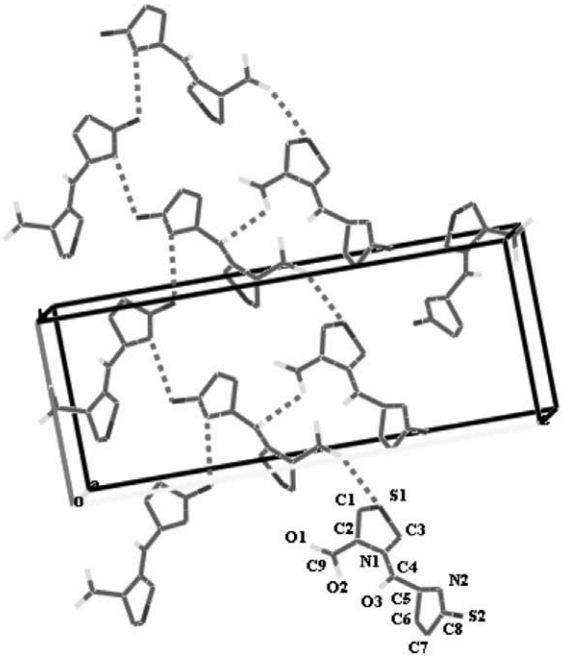

Fig. 4. Crystal packing of compound **2** showing in dotted lines the H-bond interactions (for sake of clarity only the donor and acceptor atoms are reported).

3. Experimental

3.1. X-ray crystallography

Crystals suitable for X-ray analysis were obtained from an ethanol solution as white platelets. The intensity data were collected on a CAD4 diffractometer with graphite monochromated Mo$K\alpha$ radiation (λ

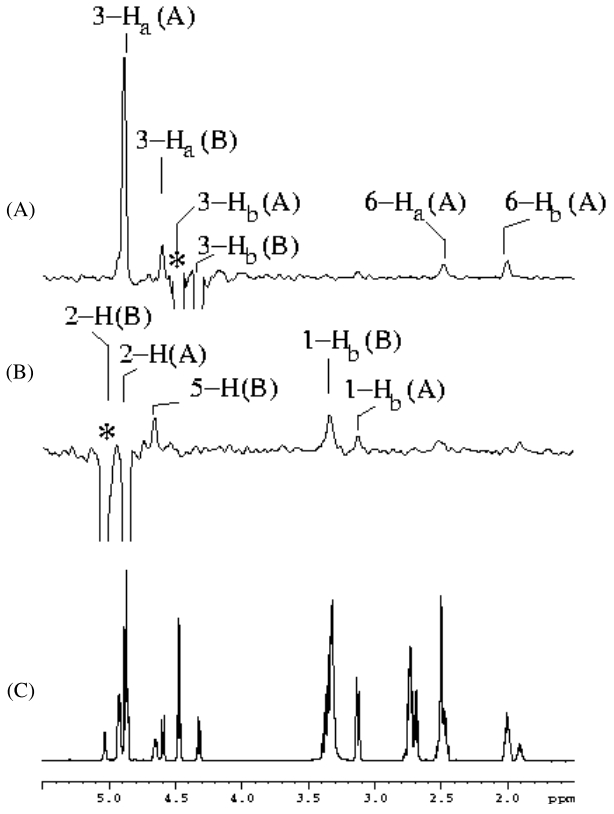

Fig. 5. Selected traces of the 600 MHz phase-sensitive 2D-NOESY spectrum ($t_{mix} = 0.4$ s) of compound **2** in DMSO-d_6. Diagonal peaks are marked with an asterisc. (A) trace at 4.47 ppm, corresponding to 3-H_b of conformer A; (B) trace at 5.03 ppm corresponding to 2-H in conformer B; (C) 1D spectrum.

Fig. 6. Cis (left) and trans (right) structures resulting from conformational analysis.

0.71073 Å). The cell parameters were determined and refined by least-squares fit of 20 high angle reflections. The structure was solved by direct methods using Sir-92 [6] and conventional Fourier synthesis (SHELX-97 [7]). The refinement of the structure was made by full matrix least-squares on F^2. All non-H-atoms were refined anisotropically. The H-atoms positions were detected in a difference Fourier and refined with isotropic thermal factors. Crystal data and a summary of the structure refinement is shown in Table 2. In Table 3, are reported the atomic fractional coordinates and in Table 4 bonds distances and angles. The supplementary crystallographic data have been deposited at the Cambridge Crystallographic Data Centre (CCDC deposition number 199343).

Table 2
Crystal data and structure refinement for **2**

Empirical formula	$C_9H_{12}N_2O_3S_2$
Formula weight	260.33
Temperature (K)	293(2)
Wavelength (Å)	0.71073
Crystal system	Orthorhombic
Space group	$P2_12_12_1$
Unit cell dimensions	
a (Å)	5.505(1)
b (Å)	9.058(1)
c (Å)	23.138(2)
Volume (Å^3)	1153.8(3)
Z, calculated density (mg/m^3)	4, 1.499
Absorption coefficient (mm^{-1})	0.455
F(000)	544
Crystal size (mm)	$0.5 \times 0.8 \times 0.3$
Theta range for data collection (°)	2.86–24.96
Limiting indices	$-2 \le h \le 6$, $-1 \le k \le 10$, $0 \le l \le 27$
Reflections collected/unique	1909/1695 [R(int) = 0.0413]
Completeness to theta	24.96 (99.8%)
Refinement method	Full-matrix least-squares on F^2
Data/restraints/parameters	1695/0/193
Goodness-of-fit on F^2	1.074
Final R indices [$I > 2\sigma(I)$]	$R_1 = 0.0292$, $wR_2 = 0.0727$
R indices (all data)	$R_1 = 0.0558$, $wR_2 = 0.0821$
Absolute structure parameter	0.06(11)
Largest difference peak and hole (e A^{-3})	0.284 and −0.301

3.2. NMR experiments

The NMR spectra were recorded at room temperature on Bruker AMX600 and AMX300 Avance spectrometers. The chemical shifts were measured in ppm and referenced to internal Me_4SI (TMS). Estimated accuracy ±0.01 ppm. Coupling constants were measured in Hz and are accurate within 0.2 Hz. The solvent used was DMSO-d_6. Concentration was 10 mg/ml. 2D-NOESY spectra were acquired at 600 MHz in the phase-sensitive TPPI mode with $2K \times 1024$ complex FIDs, spectral width of 8300 Hz, recycling delay of 2 s, 16 scans. Mixing times ranged from 0.1 to 0.4 s. All spectra were transformed and weighted with a 90° shifted sine-bell squared function to $2K \times 2k$ real data points. 2D-TOCSY and COSY double-quantum-filtered spectra were acquired and processed with similar parameters. Heteronuclear correlation spectra were acquired at 300 MHz in reversed mode. $256 \times 1k$ FIDs were acquired using standard parameters with BB 1H-decoupling, eight scans, recycling delay 3 s. The spectra were

Table 3
Atomic fractional coordinates ($\times 10^4$) and equivalent isotropic displacement parameters ($A^2 \times 10^3$) for **2**

x	y	z	U(eq)	
S(1)	7089(2)	6643(1)	6056(1)	59(1)
S(2)	−1345(2)	675(1)	7674(1)	43(1)
O(1)	3715(10)	5443(3)	4601(1)	116(2)
O(2)	5076(5)	3457(3)	5036(1)	56(1)
O(3)	1018(4)	2777(2)	5978(1)	41(1)
N(1)	4113(4)	4368(3)	6084(1)	29(1)
N(2)	2286(5)	2072(3)	7166(1)	34(1)
C(1)	4108(8)	6850(4)	5743(2)	47(1)
C(2)	3252(7)	5299(3)	5615(1)	35(1)
C(3)	6327(7)	4897(3)	6386(2)	40(1)
C(4)	2934(6)	3126(3)	6220(1)	29(1)
C(5)	3964(7)	2111(3)	6683(1)	34(1)
C(6)	3964(7)	490(4)	6482(2)	41(1)
C(7)	1687(9)	−170(4)	6743(2)	47(1)
C(8)	911(6)	898(3)	7200(1)	32(1)
C(9)	4067(8)	4755(3)	5024(1)	48(1)

U(eq) is defined as one-third of the trace of the orthogonalized *Uij* tensor.

Table 4
Bond lengths (Å) and angles (°) for **2**

Bond lengths	
S(1)–C(1)	1.803(4)
S(1)–C(3)	1.806(3)
S(2)–C(8)	1.670(3)
O(1)–C(9)	1.177(4)
O(2)–C(9)	1.300(4)
O(3)–C(4)	1.235(4)
N(1)–C(2)	1.453(4)
N(1)–C(3)	1.486(4)
N(1)–C(4)	1.337(4)
N(2)–C(5)	1.450(4)
N(2)–C(8)	1.308(4)
C(2)–C(1)	1.511(5)
C(2)–C(9)	1.520(4)
C(4)–C(5)	1.522(4)
C(6)–C(5)	1.540(4)
C(6)–C(7)	1.514(5)
C(8)–C(7)	1.496(5)
Bond angles	
C(1)–S(1)–C(3)	92.8(2)
C(4)–N(1)–C(2)	120.4(3)
C(4)–N(1)–C(3)	123.9(2)
C(2)–N(1)–C(3)	115.6(2)
C(8)–N(2)–C(5)	115.8(3)
O(3)–C(4)–N(1)	121.5(3)
O(3)–C(4)–C(5)	118.9(3)
N(1)–C(4)–C(5)	119.6(3)
N(1)–C(2)–C(1)	106.9(3)
N(1)–C(2)–C(9)	112.8(2)
C(1)–C(2)–C(9)	112.7(3)
C(7)–C(6)–C(5)	104.8(3)
N(2)–C(8)–C(7)	108.6(3)
N(2)–C(8)–S(2)	124.6(2)
C(7)–C(8)–S(2)	126.8(2)
N(2)–C(5)–C(4)	108.6(2)
N(2)–C(5)–C(6)	102.1(2)
C(4)–C(5)–C(6)	111.3(3)
C(8)–C(7)–C(6)	105.2(3)
O(1)–C(9)–O(2)	124.5(3)
O(1)–C(9)–C(2)	121.8(3)
O(2)–C(9)–C(2)	113.6(3)
N(1)–C(3)–S(1)	105.8(2)
C(2)–C(1)–S(1)	105.4(2)

transformed and weighted with a 90° shifted sine-bell squared function to 1K × 512 real data points. ^{1}H and ^{13}C resonances were attributed by means of standard homonuclear (2D-COSY-dQF and TOCSY) and heteronuclear (HMQC) correlation experiments performed at 300 and 600 MHz. Due to some overlapping of part of the spin-system, the heteronuclear correlation experiment was found particularly useful for the identification of methylene groups. All protons residing on the thiazolidinic ring were identified by the TOCSY correlation arising from the N2–H proton, resonating at 10.28 ppm. C3–$H_{a,b}$ were easily identified by the characteristic AX spin system. The identification of the remaining C2–H,C1–$H_{a,b}$ spin system follows from the analysis of the remaining protons in the 2D-COSY-dQF spectrum. The analysis of the anti-phase multiplicities in the double quantum-filtered COSY spectrum allowed also a first assignment of the relative magnitudes of coupling constants, whose values were then measured on a resolution-enhanced monodimensional spectrum taken at 600 MHz. The *J* values reported in Table 1 are not corrected for second-order effects.

3.3. Molecular modeling

The conformational analysis in water was carried out with the protocol SIMMOM [8] (Surface Integrated Molecular Orbital Molecular Mechanics QM/MM) using the programs TINKER [9] for the solvent and GAMESS [10] for the solute, starting from the crystallographic coordinates of **2**. The compound was also analyzed in vacuum (GAMESS) using the protonated carboxylic moiety in order to have a good comparison with the ^{1}H and ^{13}C NMR spectra in DMSO.

Acknowledgements

This work was financially supported by the Ministero dell'Istruzione, dell'Università e della Ricerca (MIUR), and by the University of Milano (FIRST).

References

[1] A. Pugliese, A.M. Pollono, C. Uslenghi, L. Marinelli, B. Forno, R. Girardello, Ex vivo evalutation of Pidotimod effect on immune response, Pharm. Res. 26 (Suppl 2) (1992) 178–179.
[2] (a) R.A. Chercasov, G.A. Kutyrev, A.N. Padovik, Organothiophosphorus reagents in organic synthesis, Tetrahedron 41 (1985) 2567–2624;
(b) EPXXDW EP 439044 A1 19910731.
[3] N.P. Cummings, M.J. Pabst, R.B. Johnston, Jr., Activation of macrophages for enhanced release of superoxide anion and greater killing of Candida albicans by injection of muramide dipeptide, J. Exp. Med. 152 (1980) 1659–1661.
[4] G. Alagona, C. Ghio, V. Villani, Basis set, level, and continuum solvation effects on the stability of a synthetic dipeptide: PIDOTIMOD, J. Phys. Chem. 103 (29) (1999) 5823–5832.
[5] D.J. Ayala, G. Bombieri, T. Perosino, R. Stradi, 3-(5-Oxo-l-prolyl)-l-thiazolidine-4-carboxylic acid, Acta Crystallogr. C51 (1995) 473–475.
[6] A. Altomare, M.C. Burla, M. Camalli, G. Cascarano, C. Giacovazzo, A. Gagliardi, G. Polidori, SIR92-a program for automatic solution of crystal structures by direct methods, J. Appl. Crystallogr. 27 (1994) 435.
[7] G.M. Sheldrick. SHELX-97 Program for the Refinement of Crystal Structures, University of Göttingen, Germany.

[8] J.R. Shoemaker, L.W. Burggraf, M.S. Gordon, SIMOMM: An Integrated Molecular Orbital/Molecular Mechanics Optimization Scheme for Surface, J. Phys. Chem. A 103 (1999) 3245–3251.
[9] (a) J.W. Ponder, F.M. Richards, An efficient newton-like method for molecular mechanics energy minimization of large molecules, J. Comp. Chem. 8 (1987) 1016–1024;
(b) C.E. Kundrot, J.W. Ponder, F.M. Richards, Algorithms for calculating excluded volume and its derivatives as a function of molecular conformation and their use in energy minimization, J. Comp. Chem. 12 (1991) 402–409.
[10] M.W. Schmidt, K.K. Baldridge, J.A. Boatz, S.T. Elbert, M.S. Gordon, J.H. Jensen, S. Koseki, N. Matsunaga, K.A. Nguyen, S. Su, T.L. Windus, M. Dupuis, General atomic and molecular electronic structure system, J. Comp. Chem. 14 (1993) 1347–1363.
[11] C.K. Johnson, ORTEP 11, Report ORNL-5138, Oak Ridge National Laboratory, TN (1976).
[12] G. Alagona, C. Ghio, V. Villani, Basis set, level, and continuum solvation effects on the stability of a synthetic dipeptide: PIDOTIMOD, J. Phys. Chem. 103 (1999) 5823–5832.